Accepted Manuscript

A dual-signal amplification strategy for kanamycin based on ordered mesoporous carbon-chitosan/gold nanoparticles-streptavidin and ferrocene labelled DNA

Falan Li, Xiangyou Wang, Xia Sun, Yemin Guo, Wenping Zhao

PII: S0003-2670(18)30702-5

DOI: 10.1016/j.aca.2018.05.070

Reference: ACA 236007

To appear in: *Analytica Chimica Acta*

Received Date: 9 March 2018

Revised Date: 23 May 2018

Accepted Date: 26 May 2018

Please cite this article as: F. Li, X. Wang, X. Sun, Y. Guo, W. Zhao, A dual-signal amplification strategy for kanamycin based on ordered mesoporous carbon-chitosan/gold nanoparticles-streptavidin and ferrocene labelled DNA, *Analytica Chimica Acta* (2018), doi: 10.1016/j.aca.2018.05.070.

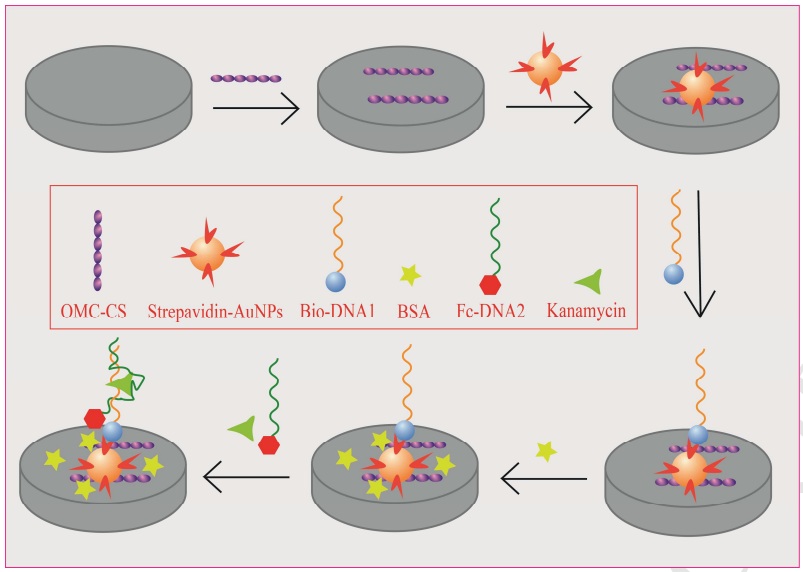

A dual-signal amplification strategy for kanamycin based on ordered mesoporous carbon-chitosan/gold nanoparticles-streptavidin and ferrocene labelled DNA

Falan Li [1, 2], Xiangyou Wang [1*, 2], Xia Sun [1*], Yemin Guo [1], Wenping Zhao [1]

[1]*School of Agricultural Engineering and Food Science, Shandong University of Technology, No. 12 Zhangzhou Road, Zibo 255049, Shandong Province, P. R. China*

[2]*School of Engineering, Northeast Agricultural University, No. 59 Mucai Street Xiangfang District, Harbin 150000, Heilongjiang Province, P. R. China*

[*] Corresponding author: Professor Xiangyou Wang and Professor Xia Sun.
Tel./Fax: +86 533 2780897
E-mail address: wxy@sdut.edu.cn (X. Wang), sunxia2151@sina.com (X. Sun)

Abstract

An ultrasensitive electrochemical aptasensor for kanamycin (KAN) detection was constructed with a dual-signal amplification strategy. The aptasensor achieved greatly amplified sensitivity due to the excellent electrical conductivity of the ordered mesoporous carbon-chitosan (OMC-CS)/gold nanoparticles-streptavidin (AuNPs-SA) and DNA2 labelled with ferrocene (Fc-DNA2). The AuNPs-SA was used to immobilize the DNA strand (biotin labelled) with the biotin-streptavidin system. The DNA2 strand containing the KAN aptamer was labelled with ferrocene to increase the current signal on the electrode surface when bound to KAN. Some factors that affect the performance of the aptasensor were optimized, and the proposed aptasensor provided a wide linear range from 1×10^{-10} M to 4×10^{-6} M, with a detection limit as low as 35.69 pM for KAN under the optimized conditions. This aptasensor had satisfactory electrochemical performance with good stability, sensitivity and reproducibility. Additionally, it also displayed a good specificity for KAN without interference from competitive analogues. Furthermore, the constructed aptasensor was successfully used to detect KAN in a real milk sample. The proposed method for KAN detection has great potential for the detection of other antibiotics.

Keywords: Dual-signal amplification strategy; gold nanoparticles-streptavidin; biotin; ferrocene; aptasensor.

Introduction

Kanamycin (KAN) is an important antibiotic derived from *Streptomyces Kanamyceticus* [1-2], which has been extensively used in the treatment of Gram-positive and Gram-negative bacterial infections in human and animal [3]. KAN residue in food causes serious side effects, such as nephrotoxicity, ototoxicity and antibiotic resistance [4]. To ensure the food safety and quality, the European Union determined that the maximum residue limit of KAN acceptable in milk is 150 μg/kg (257.4 nM) [5]. Accordingly, sufficiently sensitive methods for detection of KAN in milk are necessary to ensure the safety of products for human consumption and thus our health. Recently, many analytical methods have been used to detect the KAN such as gas chromatography [6], capillary electrophoresis (CE) [7], high-performance liquid chromatography (HPLC) [8], solid-phase extraction (SPE) [9], immunoassays [10-11], enzyme-linked immunosorbent assay (ELISA) [12] and colloidal gold test strips [13]. However, most of these above-mentioned methods are still limited in application due to the high turnaround time, expensive equipment, complex operation, and tedious sample pretreatment. Therefore, new strategies for sensitive and selective KAN detection are still desired.

Aptamers are obtained by in vitro screening [14-15], and can bind to target molecules with high affinity and selectivity for artificial single-stranded DNA or RNA molecules [16-18]. Aptamers have attracted enormous interest in biosensor design due to advantages like excellent stability, low toxicity and ease of synthesis and modification [19-21]. In view of the obvious advantages of aptamers [22], numerous

aptasensors have been proposed for use in the fields of clinical diagnosis and food safety, based on colorimetric [23], electrochemical [24], fluorescence [25], chemiluminescence [26], and cantilever array [27] detection.

To improve the analytical performance of electrochemical biosensor, various nanomaterials have been used in their fabrication [28-30]. Ordered mesoporous carbon (OMC) materials have drawn attention due to their large specific surface area, good conductivity and good biocompatibility [31-35]. Moreover, OMC materials can provide an excellent microenvironment for biomolecules such as DNA and proteins [36], and their high-density edge sites provide a number of favorable sites for electron transport [37]. However, the film forming ability of OMC materials is poor, and thus an additional film-forming material such as chitosan (CS), is required to help form the film. CS is widely used as an immobilization matrix due to its advantages, such as low cost, non-toxicity, antibacterial activity, biocompatibility and biodegradability [38-39]. Gold nanoparticles (AuNPs) are also widely used to construct aptasensors due to their unique properties, including ease of synthesis, high conductivity, and easy control over electrode microenvironment [40-42]. The gold nanoparticles are labelled with streptavidin, which can bind to biotin with high specific affinity (affinity constant up to 10^{15} mol/L) and have high conductivity. Due to this affinity, the method involving the streptavidin-biotin reaction has been widely used [43]. The aptamer is usually labelled with biotin, and then binds with high affinity to the streptavidin that is adsorbed to the electrode to immobilize the aptamer on the electrode [44]. The biotin-labelled DNA1 strand binds to the streptavidin-labelled AuNPs through the

high affinity binding between streptavidin and biotin. The ferrocene-label DNA2 (Fc-DNA2) strand containing the KAN aptamer specifically binds to the KAN and DNA1 and increases the current signal on the electrode surface. The electrochemical current signal of ferrocene would increase with the increase of the KAN concentration. Here, the functional metal nanoparticles play a dual role in providing signal and recognition target, which makes the detection method step simple and highly sensitive.

The purpose of this work is to develop a sensitive and simple method for detecting KAN in milk. A novel electrochemical aptasensor based on ordered mesoporous carbon-chitosan (OMC-CS), gold nanoparticles-streptavidin (AuNPs-SA) and Fc-DNA2 strand was designed for selective and sensitive detection of KAN. The OMC-CS and AuNPs-SA nanocomposites form a strong conductive pathway for electron transfer. The DNA2 strand containing the KAN aptamer is labelled with ferrocene to increase the current signal on the electrode surface when bound to KAN. The proposed aptasensor has a lower detection limit with a wide linear range for KAN, and was successfully applied to milk samples. To the best of our knowledge, there has been no report on aptasensor for KAN detection in the literature.

Experimental

Reagents and chemicals

The OMC was obtained from Yoshikura nanotechnology Co., Ltd. (Nanjing, China). The AuNPs-SA (20 nm) was purchased from RuiXi Biological Technology Co., Ltd. (Xi'an, China). Kanamycin (KAN), tobramycin, streptomycin, and neomycin

were all obtained from Jingchun Co., Ltd. (Tianjing, China). A long strand of DNA that contains the KAN aptamer labelled with ferrocene (Fc-DNA2, 5'-ACTTCTCGCAAGATGGGGGTTGAGGCTAAGCCGAATACTCCAGT-Fc-3') and the complementary strand of the long strand of DNA labelled with biotin (Bio-DNA1, 5'-Bio-ACTGGAGTATTGCGAGAAGT-3') were purchased from Sangon Biotechnology (Shanghai, China).

Apparatus

A three-electrode system was used, which consisted of an auxiliary electrode (platinum wire), a reference electrode (Ag/AgCl) and a working glassy carbon electrode (GCE, D=3 mm), in CHI 660D electrochemical workstation (Shanghai, China) for all electrochemical measurements. The morphology of the nanocomposites was characterized using a Tecnai G2F20S-TWIN transmission electron microscope and Sirion 200 field emission scanning electron microscope (FEI, Hillsboro, OR, USA).

Preparation of OMC-CS

CS was dissolved in 2.0 M acetic acid solution and then magnetically stirred for 8 h or more to obtain a 0.2% CS solution (4 ml, w/v). The pH was adjusted with a NaOH solution to pH 5.0. Then, after adding 2 mg of OMC to the above solution it was sonicated for 1 h until the solution reached a homogeneous stable state. The obtained highly dispersed solution indicated that the OMC-CS suspension had been successfully prepared.

Determination of dissociation constant (Kd)

To determine the binding affinity of the selected aptamer, A fixed concentration of KAN was incubated with increasing concentration of KAN aptamer under mild shaking conditions for 30 min. The unbound KAN aptamer was removed by two gentle washes with selection buffer. The dissociation constant (Kd) value was calculated by employing the nonlinear regression analysis using electroanalytical techniques.

$$\frac{i}{\Delta i} = \frac{1}{\Delta i_{\max}} + \frac{1}{K_d \Delta i_{\max} [B]}$$

where [B] is the concentration of the target (KAN) in solution, Kd is the dissociation constant for the aptamer/KAN binding, Δi is the variation of the current, and Δimax is the maximum variation obtained corresponding to saturation.

Construction of the aptasensor

The bared electrode was first polished with 0.05 μm alumina powder and then washed ultrasonically in ethanol, nitric acid and double distilled water. The electrodes were cyclically scanned (-0.1-+1.0 V) and placed in 0.5 M H_2SO_4 solution for activation. Then, 7 μL of the CS-OMC suspension was added dropwise onto the electrode surface. After the electrode was dried, 7 μL of the AuNPs-SA solution was added onto its surface. Subsequently, the dried modified electrode was incubated in Bio-DNA1 for 0.5 h. Afterwards, the electrode was immersed in 0.5% bovine serum albumin (BSA) to block non-specific sites. Ultimately, the solution of Fc-DNA2 and KAN was added dropwise onto the electrode, which was then rinsed with PBS to remove unbound DNA. The schematic illustration of the aptasensor assembled

procedure is depicted in Fig. 1.

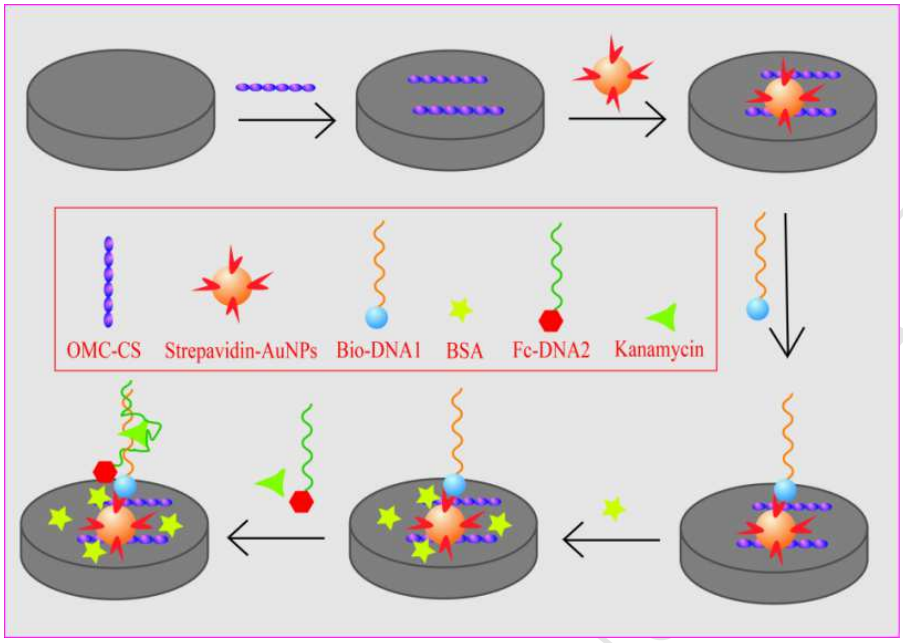

Fig. 1. The schematic illustration of the aptasensor assembled procedure.

Electrochemical assay of KAN

The electrochemical signals of the cyclic voltammetry (CV) and differential pulse voltammetry (DPV) were all measured in electrolyte solution (0.1 M KCl, 5 mM $[Fe(CN)_6]^{4-/3-}$) with scanning potentials of -0.6- +0.1 V and 0.0 V - +0.4 V, respectively.

Sample preparation

The KAN-free milk was first diluted with PBS (pH 7.5), then centrifuged for 10 min (10,000 rpm) and allowed to stand for 10 min. The supernatant of the milk was collected and filtered through a 0.22 μm sterile Millipore membrane, then the KAN standard solution was added to the prepared sample solutions of different KAN concentrations.

Results and discussion

Dissociation constant (Kd) measurement

The calculated Kd value obtained of KAN-aptamer is 0.043 nM. The aptamer showed high affinity to KAN, which would enhance the sensitivity of kanamycin detection methods.

Characterization of the nanomaterials

The morphologies of the OMC-CS and SA-AuNPs composites were examined using scanning electron microscopy (SEM) and transmission electron microscopy (TEM), respectively. The image shown in Fig. 2 (a) reveals that the OMC-CS is composed of numerous uniformly and orderly-distributed rod-like particles. These particles allow the OMC-CS to possess a high porosity and surface area to provide a better protective microenvironment for the aptamer. The SEM image of AuNPs-SA (Fig. 2 (b)) shows that the AuNPs were separated from each other in the presence of streptavidin molecules. The image presented in Fig. 2 (c) reveals that the AuNPs were successfully labelled with streptavidin. When biotin was added, AuNPs were aggregated through high affinity interaction between streptavidin and biotin (Fig. 2 (d)).

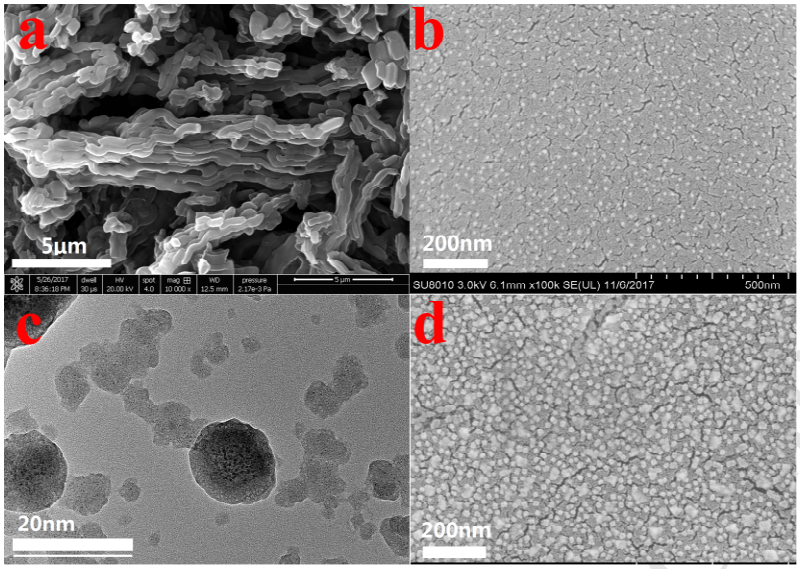

Fig. 2. (a) SEM images of OMC-CS; (b) SEM images of SA-AuNPs; (c) TEM images of SA-AuNPs+Bio-DNA1; (d) SEM images of SA-AuNPs+Bio-DNA1.

Electrochemical characterization of the aptasensor

The formation process of the aptasensor was characterized using CV (Fig. 3). Due to the oxidation-reduction reaction on the probe ($[Fe(CN)_6]^{4-/3-}$), the CV of the bare GCE showed a pair of distinct redox peaks (curve a). With the addition of OMC-CS, the peak current was significantly increased due to the high conductivity of OMC-CS (curve b). Since the AuNPs-SA composites also have excellent conductivity, the peak current of the AuNPs-SA/OMC-CS/GCE showed a higher current after the addition of the AuNPs-SA composites (curve c). The results showed that the OMC-CS and AuNPs-SA composites provided effective electron transporting ability for this aptasensor. When the Bio-DNA1 was immobilized onto the AuNPs-SA/OMC-CS/GCE surface, the peak current was significantly reduced due to the non-conductive nature of oligonucleotides (curve d). When the electrode was soaked in a BSA solution, the current was further decreased due to the formation of an

isolating layer of BSA that successfully blocked the adsorption to non-specific sites (curve e). The amperometric current was increased when Fc-DNA2 was added (curve f). Since the complementary probe (DNA2) was labelled with ferrocene, the ferrocene could approach the electrode surface to exchange electron and generate high current when the Fc-DNA2 hybridizes with DNA1 to form a duplex. Finally, the amperometric was current further increased when KAN was added (curve g). Since the combination of aptamer and target made the DNA chain more tightly connected, making the three level structure of them more firmly combined, making Fc closed to the electrode surface.

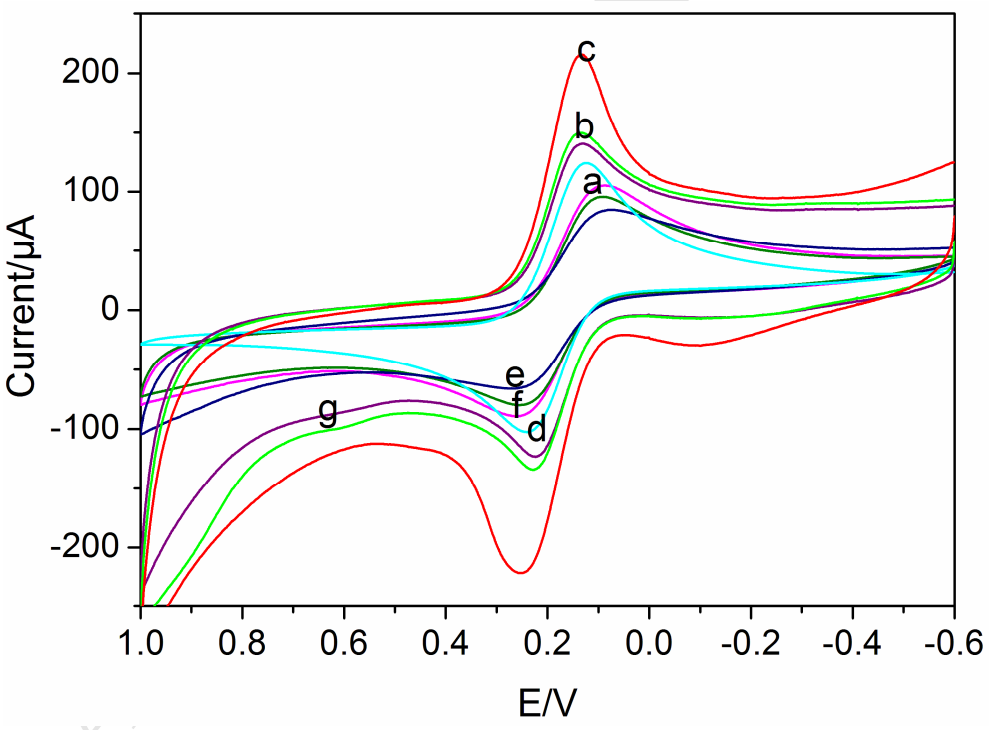

Fig. 3. CV: (a) bare GCE, (b) OMC-CS/GCE, (c) SA-AuNPs/OMC-CS/GCE, (d) Bio-DNA1/SA-AuNPs/OMC-CS/GCE, (e) BSA/Bio-DNA1/SA-AuNPs/OMC-CS/GCE, (f) Fc-DNA2/BSA/Bio-DNA1/SA-AuNPs/OMC-CS/GCE, (g) KAN/Fc-DNA2/BSA/Bio-DNA1/SA-AuNPs/OMC-CS/GCE.

Optimization the performance of aptasensor

In order to achieve a satisfactory detection performance, the effect of several factors, including the DNA1 concentration, DNA2 concentration, pH value of the working solution and incubation time, were investigated and optimized. As shown in Fig. 4 (a-b), DNA1 and DNA2 at different concentrations were selected to examine the effect of the aptamer concentration on the current signal. As anticipated, the current difference (ΔI) was increased with the increase of the concentration of either DNA1 or DNA2, and the ΔI reached the maximum value at a DNA concentration of 20 μM. Thus, 20 μM was the optimal concentration of DNA1 or DNA2 used for the aptasensor fabrication. The effect of pH on the aptasensor response was also studied with a different pH electrolyte solution (6.0-7.8). The ΔI initially increased and then decreased with the increase of the pH value, and the maximum ΔI value was obtained at pH 7.5 (Fig. 4 (c)). Thus, 7.5 was selected as the pH of the electrolyte solution used in the construction of the aptasensor. The incubation time during the functionalization was also investigated with the aim of achieving a fast detection. A series of BSA/Bio-DNA1/AuNPs-SA/OMC-CS/GCE were incubated for 60, 80, 100, 110, 120, 130, 140 and 160 min. As shown in Fig. 4 (d), the active sites for KAN binding appear to have reached saturation after 120 min, as the ΔI increased with time until it became stable after 120 min. Therefore, the optimal incubation time of 120 min was chosen for subsequent experiments.

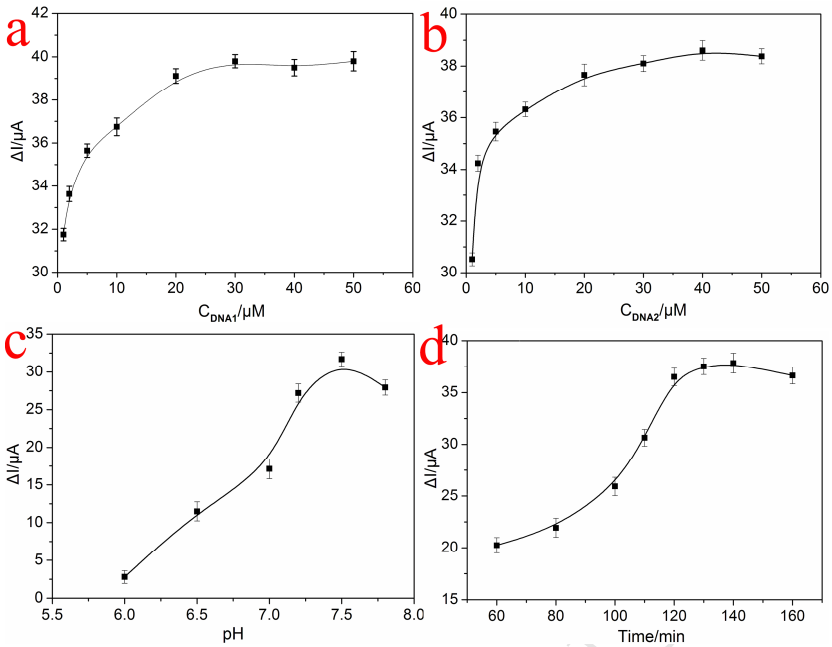

Fig. 4. Effect of experimental conditions: (a) the concentration of DNA1, (b) the concentration of DNA2, (c) pH of the electrolyte solution, (d) the incubation time of DNA1.

In order to gain an insight into the influence of the interaction between the four test conditions on the detection performance of the aptasensor, a combination of the results of single factor test with those of the quadratic orthogonal rotation test was used to optimize the experimental conditions. The coded independent variables (X_1, X_2, X_3, X_4) and uncoded variables (X_1 = inhibition time/min, X_2 = pH of the bottom, X_3 = concentration of DNA1/μM and X_4 = concentration of DNA2/μM) with their variation levels are shown in Table S1. The arrangements of the test and response results are shown in Table S2.

Table S1 Test factors and levels.

Independent variables	Levels of variation				
	-2	-1	0	1	2
X_1 = inhibition time/min	80	100	120	140	160
X_2 = pH of the bottom	6.9	7.2	7.5	7.8	8.1
X_3 = concentration of	10	15	20	25	30
X4=concentration of	10	15	20	25	30

245 Table S2 Quadratic orthogonal rotation combination design and response.

Assay	Independent variable coded				Response
	X_1	X_2	X_3	X4	Current difference/μA
1	1	1	1	1	30.77
2	1	1	1	-1	30.54
3	1	1	-1	1	30.02
4	1	1	-1	-1	28.87
5	1	-1	1	1	29.43
6	1	-1	1	-1	31.29
7	1	-1	-1	1	27.60
8	1	-1	-1	-1	26.10
9	-1	1	1	1	27.23
10	-1	1	1	-1	26.97
11	-1	1	-1	1	26.59
12	-1	1	-1	-1	25.90
13	-1	-1	1	1	13.04
14	-1	-1	1	-1	12.47
15	-1	-1	-1	1	12.89
16	-1	-1	-1	-1	12.21
17	2	0	0	0	12.50
18	-2	0	0	0	37.48
19	0	2	0	0	15.17
20	0	-2	0	0	23.52
21	0	0	2	0	37.69
22	0	0	-2	0	40.50
23	0	0	0	2	35.97
24	0	0	0	-2	38.40
25	0	0	0	0	44.37
26	0	0	0	0	47.79
27	0	0	0	0	46.26
28	0	0	0	0	44.88
29	0	0	0	0	48.40
30	0	0	0	0	45.96
31	0	0	0	0	50.46
32	0	0	0	0	46.88
33	0	0	0	0	48.94
34	0	0	0	0	46.52
35	0	0	0	0	47.24
36	0	0	0	0	45.69

246 The response surfaces of the test results are shown in Fig. 5. These results reveal

247 that with the increase of the pH value, the response current initially increased and then

decreased, the maximum ΔI occurred at pH 7.5. Meanwhile, with the increase of the concentration of DNA1 and DNA2, the ΔI of response also initially increased and tended to be stable up to the concentration of 20 μM. This might be due to the limited electrode area leading to excessive accumulation of DNA, which thus hinders the electron transfer of the electrode surface. In addition, when the incubation time of DNA1 exceeded 120 min, the ΔI decreased slightly, but the basic trend was almost stable. Overall, the test results did not change compared to the single condition control.

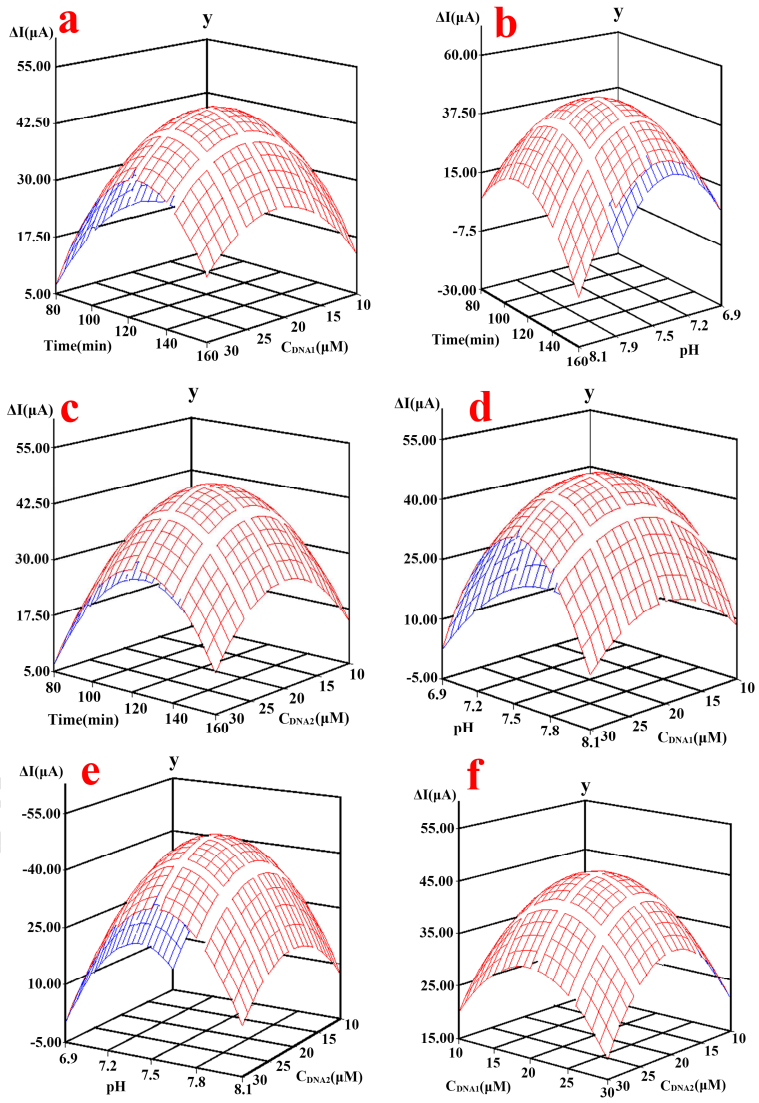

Fig. 5. Response surface of parameter optimization in orthogonal experiment.

Electrochemical detection of KAN

Under optimal conditions, a series of KAN standard solutions at different concentrations were studied by DPV to investigate the analytical capabilities of the developed aptasensor. KAN can bind the aptamer with higher affinity, and the part strand of DNA1 and Fc-DNA2 that are complementary to it can hybridize to it. The results revealed that as the concentrations of KAN and Fc-DNA2 increased, a larger surface area of the ferrocene became exposed. Thus, the peak current detected by DPV gradually increased with the increase of the concentration of KAN (Fig. 6). In the range from 100 pM to 1 μM, the linear analysis of KAN generated the following equation: y =-13.6661+8.1338x, and a correlation coefficient of 0.9893. The detection limit was determined to be 35.69 pM (S/N = 3), which is much lower than the concentration the European Union determined to be maximum KAN maximum acceptable contamination level (257.4 nM) in milk [5]. Compared to the previously reported methods [45-51], the method developed here is superior with respect to its detection limit, and it is rapid and facile (Table 1).

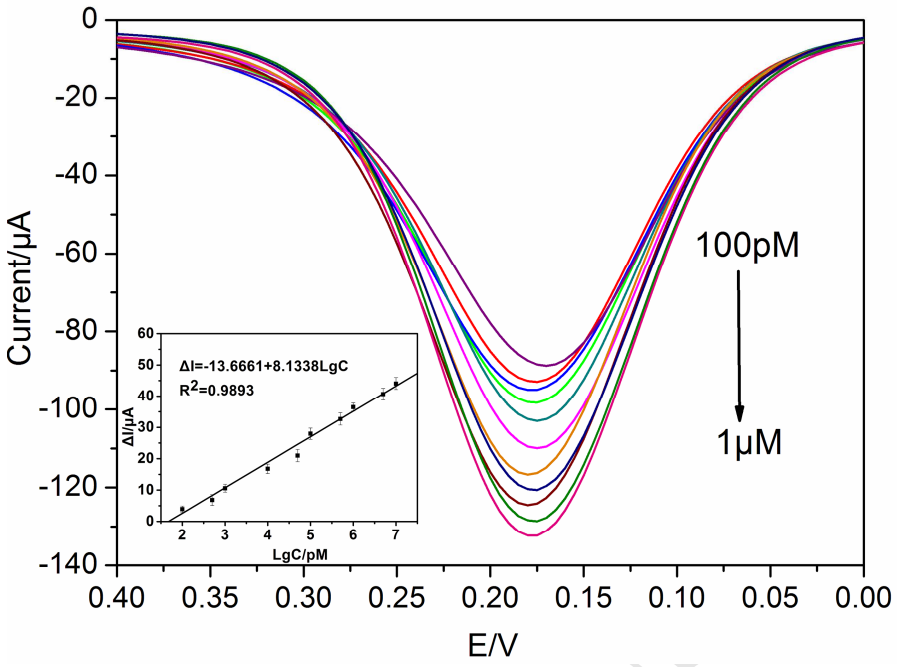

Fig. 6. DPV responses to different concentrations of KAN (1×10^{-10} to 1×10^{-6} M), the inset describes calibration curve for KAN detection.

Table 1 Comparison with other KAN detection methods

Detection method	Linear range (nM)	Limit of detection (nM)	References
Colorimetry	85.83-103.00	4.5	[42]
Colorimetry	5-100 100-2×10^4	4	[43]
Fluorescence	2-60	0.612	[44]
Spectrophotometric	1–500	1	[45]
ELISA	-	1.76	[46]
Photoelectrochemical aptasensor	1-230	0.2	[47]
Electrochemical aptasensor	1-1×10^5	0.87	[48]
Electrochemical aptasensor	0.1-1000	0.03569	This work

Specificity, stability, reproducibility and regeneration of the aptasensor

Selectivity is one of the important factors which had been tested in this work to evaluate the performance of the developed biosensor. A KAN solution of 100 nM, containing 10 μM of other antibiotics (streptomycin (STR), gentamicin (GEN), neomycin (NEO), tobramycin (TOB) and oxytetracycline (OTT)) as interferents substances, was analyzed using the aptasensor and the results are shown in Fig. 7. The

283 results reveal that the current change in the presence of these interferents was less
284 than 4.3%, which indicated that the aptasensor has a good specificity for KAN and
285 interference resistance to other antibiotics.

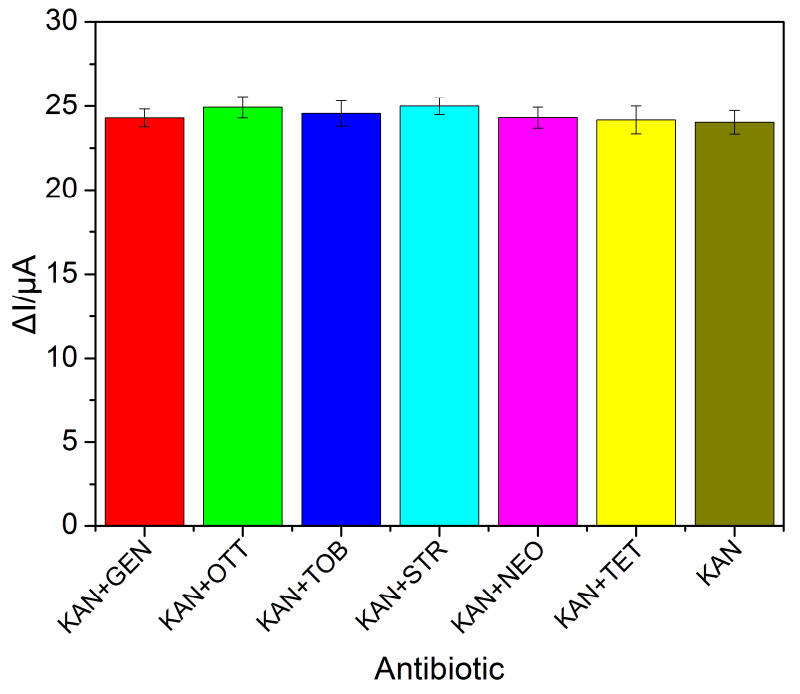

286

287 Fig. 7. Selectivity assessment of the aptasensor. KAN: kanamycin, TOB: tobramycin, GEN:
288 gentamicin, OTT: oxytetracycline, NEO: neomycin, STR: streptomycin and TET: tetracycline.

289 Reproducibility is another important factor in aptasensor performance. To
290 evaluate reproducibility, five aptasensors were prepared in the same way for the
291 detection of KAN. The calculated percent relative standard deviation (RSD) was
292 3.82%, indicating that the aptasensor-based assay had a good reproducibility.

293 To test the stability of the aptasensor, five electrodes were prepared and stored at
294 4 □ and then used to detect KAN. The results of the KAN detection analysis revealed
295 that the measurement of the same concentration decreased only 5.61% after four-week
296 storage of the aptamer, which indicated that the aptasensor had a good stability. This
297 might be due to the stability of the DNA-aptamer and the high affinity between

298 streptavidin and biotin.

299 To evaluate the regenerability of the aptasensor, the aptasensor that have been
300 used for the detection of KAN was immersed into a glycine-hydrochloric acid
301 solution (0.2 M, pH 2.0) for 1 min to break the aptamer-KAN linkage. Afterwards, the
302 aptasensors were prepared for the detection of KAN. Following the detection of KAN,
303 the aptamer-KAN complex was again immersed into the glycine-hydrochloric acid
304 solution. After five regeneration cycles, the current response of the aptasensor
305 retained about 90.41% of its original response value (with a RSD of 4.06%),
306 indicating that this aptasensor has a good regenerability.

307 **KAN detection in milk**

308 To study the applicability and precision of the developed aptasensor with real
309 samples, different concentrations of KAN were detected by the standard addition
310 methods in biological fluid (milk) samples containing various interfering substances
311 and their recoveries were calculated. The milk sample was centrifuged to remove
312 interfering substances, such as fat. The centrifugal conditions were optimized by
313 quadratic orthogonal rotation experiments. The data presented in Table S3 shows the
314 level of the experimental factors, and that in Table S4 shows the experimental
315 arrangements and results. The results presented in Fig. S1 show the response surfaces
316 of the centrifugal conditions, the optimal centrifugal speed was 10000 r/min, the
317 optimal centrifugal time and standing time were all 10 min. The aptasensor was used
318 to analyze the recorded response signals. As the data shown in Table 2 reveals, the
319 recoveries ranged from 92.86 to 104.91% with a RSD of less than 5.04%. Thus, the

320 proposed aptasensor recognized the target with high selectively and reliability even in

321 a complex biological environment like milk.

322 Table S3 Experimental factors level coding.

Independent variables	Levels of variation				
	-1.682	-1	0	1	1.682
X_1 = centrifugal	8320	900	1000	1100	1168
X2 = centrifugal time/min	5	7	10	13	15
X3 = standing time/min	5	7	10	13	15

323 Table S4 Experimental arrangements and results.

Assay	Independent variable coded			Response
	X_1	X_2	X_3	Current difference/μA
1	1	1	1	50.47
2	1	1	-1	49.68
3	1	-1	1	48.59
4	1	-1	-1	47.07
5	-1	1	1	25.28
6	-1	1	-1	24.34
7	-1	-1	1	24.07
8	-1	-1	-1	23.13
9	1.682	0	0	50.89
10	-1.682	0	0	24.23
11	0	1.682	0	51.18
12	0	-1.682	0	26.06
13	0	0	1.682	51.20
14	0	0	-1.682	40.86
15	0	0	0	50.16
16	0	0	0	51.30
17	0	0	0	50.40
18	0	0	0	50.92
19	0	0	0	49.47
20	0	0	0	50.45

324

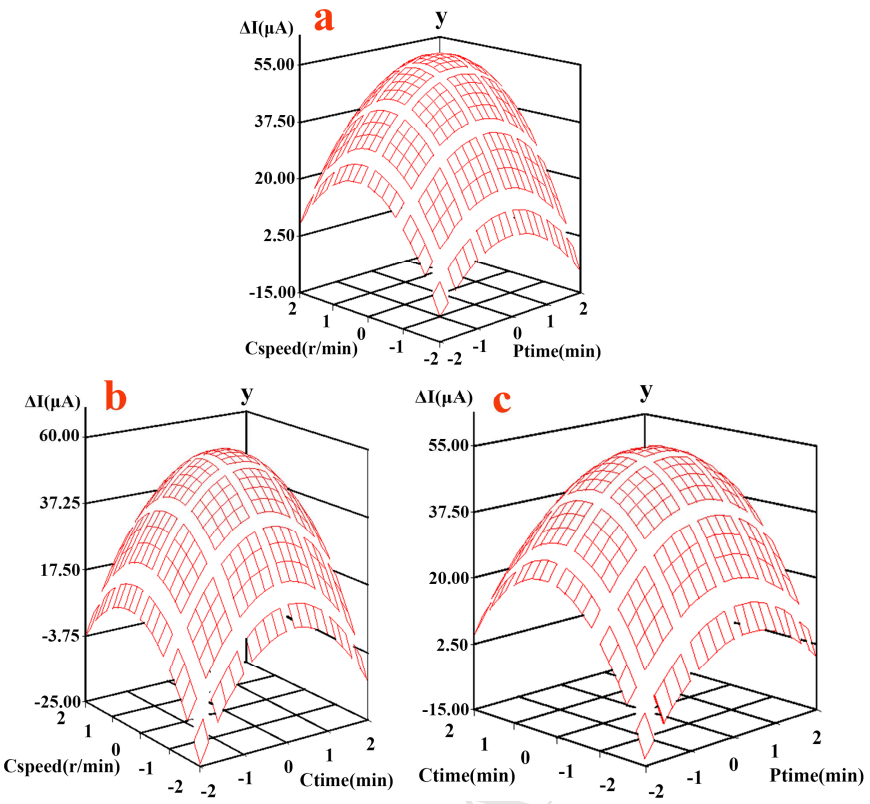

Fig. S1. Response surface of sample processing conditions orthogonal experiment.

Table 2 Recovery and RSD of KAN in spiked milk samples

Milk found(μM)	Added(μM)	Total found(μM)	Recovery（%）	RSD (%, n=3)
No detected	0.00000	0.00000	-	-
No detected	0.00500	0.00474	94.80	3.36
No detected	0.01000	0.01032	103.20	5.04
No detected	0.05000	0.04643	92.86	3.26
No detected	0.10000	0.10491	104.91	2.10
No detected	0.50000	0.52138	104.276	4.35

Conclusions

In this study, a novel aptasensor for the quantitative detection of KAN based on OMC-CS and AuNPs-SA was successfully fabricated. The OMC-CS and AuNPs-SA nanocomposite not only greatly enhanced the quantity of immobilized biomolecules, such as the aptamers, but also significantly improved the amperometric signal of the

aptasensor. The designed aptasensor showed a considerably low detection limit (35.69 pM) and a wide linear response range (1×10^{-10}-1×10^{-6} M). The developed aptasensor showed good repeatability, specificity, reproducibility, and a long-term stability of up to four weeks. The aptasensor was successfully applied for KAN detection with high a recovery ranging from 92.86 to 104.91% in complex real milk samples. It is anticipated that the application of the developed aptasensor could be further extended to simple and real-time detection of other antibiotics.

Acknowledgments

This work was supported by the National Natural Science Foundation of China (No.31471641, 31772068, 31701681), Special Project of Independent Innovation of Shandong Province (2014CGZH0703), Shandong Provincial Natural Science Foundation (ZR2014CM009, ZR2015CM016, ZR2016CM29, ZR2017BC001, ZR2014FL003), Key Research and Invention Program of Shandong Province (2017GNC10119), Key Innovative project for 2017 Major Agriculture Application Technology of Shandong Province.

References

[1] X.L. Qin, W.J. Guo, H.J. Yu, J. Zhao, M.S. Pei, A novel electrochemical aptasensor based on MWCNTs-BMIMPF6 and amino functionalized graphene nanocomposites film for determination of kanamycin, Anal. Methods. 7 (2015) 5419-5427.

[2] C.M. Spahn, C.D. Prescott, Throwing a spanner in the works: antibiotics and the translation apparatus, J. Mol. Med. 74 (1996) 423-439.

[3] D. Fourmy, S. Yoshizawa, J.D. Puglisi, Paromomycin binding induces a local conformational change in the A-site of 16 S rRNA, J. Mol. Biol. 277 (1998) 333-345.

[4] R. Oertel, V. Neumeister, W. Kirch, Hydrophilic interaction chromatography combined with tandem-mass spectrometry to determine six aminoglycosides in serum, J. Chromatogr. A. 1058 (2004) 197-201.

[5] European agency for the evaluation of medical products (EMEA) London: 2003. Regulation No. EMEA/MRL/886/03-FINAL.

[6] M. Preu, D. Guyot, M. Petz, Development of a gas chromatography-mass spectrometry method for the analysis of aminoglycoside antibiotics using experimental design for the optimisation of the derivatisation reactions, J. Chromatogr. A. 818 (1998) 95-108.

[7] E. Kaale, A.V. Schepdael, E. Roets, J. Hoogmartens, Determination of kanamycin by electrophoretically mediated microanalysis with in-capillary derivatization and UV detection, Electrophoresis 24 (2003) 1119-1125.

[8] S.H. Chen, Y.C. Liang, Y.W. Chou, Analysis of kanamycin A in human plasma and in oral dosage form by derivatization with 1-naphthyl isothiocyanate and high-performance liquid chromatography, J. Sep. Sci. 29 (2006) 607-612.

[9] J. Yang, J. Li, J. Qiao, H. Lian, H. Chen, Solid phase extraction of magnetic carbon doped Fe_3O_4 nanoparticles, J. Chromatogr. A. 1325 (2014) 8-15.

[10] Y.F. Zhao, Q. Wei, C.X. Xu, H. Li, D. Wu, Y.Y. Cai, K.X. Mao, Z.T. Cui, B. Du, Label-free electrochemical immunosensor for sensitive detection of kanamycin, Sens. Actuators B. 155 (2011) 618-625.

[11] W. Haasnoot, G. Cazemier, M. Koets, A.V. Amerongen, Single biosensor immunoassay for the detection of five aminoglycosides in reconstituted skimmed milk, Anal. Chim. Acta. 488 (2003) 53-60.

[12] E.E.M.G. Loomans, J.V. Wiltenburg, M. Koets, A.V. Amerongen, Neamin as an immunogen for the development of a generic ELISA detecting gentamicin, kanamycin, and neomycin in milk, J. Agric. Food Chem. 51 (2003) 587-593.

[13] Y. Chen, Z. Wang, Z. Wang, S. Tang, Y. Zhu, X. Xiao, Rapid enzyme-linked immunosorbent assay and colloidal gold immunoassay for kanamycin and tobramycin in swine tissues, J. Agric. Food Chem. 56 (2008) 2944-2952.

[14] X. Bai, H. Hou, B. Zhang, J. Tang, Label-free detection of kanamycin using aptamer-based cantilever array sensor, Biosens. Bioelectron. 56 (2014) 112-116.

[15] X. Tang, Y.S. Wang, J.H. Xue, B. Zhou, J.X. Cao, S.H. Chen, M.H. Li, X.F. Wang, Y.F. Zhu, Y.Q. Huang, A novel strategy for dual-channel detection of metallothioneins and mercury based on the conformational switching of functional chimera aptamer, J. Pharm. Biomed. Anal. 107 (2015) 258-264.

[16] S.C. Gopinath, Methods developed for SELEX, Anal. Bioanal. Chem. 387 (2007) 171-182.

[17] C.D. Medley, S. Bamrungsap, W. Tan, J.E. Smith, Aptamer-conjugated nanoparticles for cancer cell detection, Anal. Chem. 83 (2011) 727-734.

[18] S. Wu, H. Zhang, Z. Shi, N. Duan, C. Fang, S. Dai, Z. Wang, Aptamer-based fluorescence biosensor for chloramphenicol determination using upconversion nanoparticles, Food Control. 50 (2015) 597-604.

400 [19] A.D. Keefe, S. Pai, A. Ellington, Aptamers as therapeutics, Nat. Rev. Drug
401 Discov. 9 (2010) 537-550.
402 [20] P. Luo, Y. Liu, Y. Xia, H. Xu, G. Xie, Aptamer biosensor for sensitive detection of
403 toxin A of Clostridium difficile using gold nanoparticles synthesized by Bacillus
404 stearothermophilus, Biosens. Bioelectron. 54 (2014) 217-221.
405 [21] Q. Wei, Y.F. Zhao, B. Du, D. Wu, H. Li, M.H. Yang, Ultrasensitive detection of
406 kanamycin in animal derived foods by label-free electrochemical immunosensor,
407 Food Chem. 134 (2012) 1601-1606.
408 [22] Y.N. Hou, J.F. Liu, M. Hong, X. Li, Y.H. Ma, Q.L. Yue, C.Z. Li, A reusable
409 aptasensor of thrombin based on DNA machine employing resonance light scattering
410 technique, Biosens. Bioelectron. 92 (2017) 259-265.
411 [23] Y.P. Chen, M.q. Zou, C. Qi, M.X. Xie, D.N. Wang, Y.F. Wang, Q. Xue, J.F. Li, Y.
412 Chen, Immunosensor based on magnetic relaxation switch and biotin-streptavidin
413 system for the detection of Kanamycin in milk, Biosens. Bioelectron. 39 (2013)
414 112-117.
415 [24] S. Song, L. Wang, J. Li, C. Fan, J. Zhao, Aptamer-based biosensors, TrAC Trends
416 Anal. Chem. 27 (2008) 108-117.
417 [25] T.K. Sharma, R. Ramanathan, P. Weerathunge, M. Mohammadtaheri, H.K.
418 Daima, R. Shukla, V. Bansai, Aptamer-mediated 'turn-off/turn-on' nanozyme activity
419 of gold nanoparticles for kanamycin detection, Chem. Comm. 50 (2014)
420 15856-15859.
421 [26] R.Y. Robati, A. Arab, M. Ramezani, F.A. Langroodi, K. Abnous, S.M. Taghdisi,

422 Aptasensors for quantitative detection of kanamycin, Biosens. Bioelectron. 82 (2016)
423 162-172.
424 [27] J. Daprà, L.H. Lauridsen, A.T. Nielsen, N. Rozlosnik, Comparative study on
425 aptamers as recognition elements for antibiotics in a label-free all-polymer biosensor,
426 Biosens. Bioelectron. 43 (2013) 315-320.
427 [28] F. Long, Z. Zhang, J. Wang, L. Yan, B. Zhou, Cobalt-nickel bimetallic
428 nanoparticles decorated graphene sensitized imprinted electrochemical sensor for
429 determination of octylphenol, Electrochim. Acta. 168 (2015) 337-345.
430 [29] J.P. Wang, H. Gao, F.L. Sun, C.X. Xu, Nanoporous PtAu alloy as an
431 electrochemical sensor for glucose and hydrogen peroxide, Sens. Actuators B. 191
432 (2014) 612-618.
433 [30] H. Wang, J. Wu, J.S. Li, Y.J. Ding, G.L. Shen, R.Q. Yu, Nanogold
434 particle-enhanced oriented adsorption of antibody fragments for immunosensing
435 platforms, Biosens. Bioelectron. 20 (2005) 2210-2217.
436 [31] H. Dai, Y.Y. Lin, G.F. Xu, L.S. Gong, C.P. Yang, X.L. Ma, G.N. Chen, Cathodic
437 electrochemiluminescence of luminol using polyaniline/ordered mesoporous carbon
438 (CMK-3) hybrid modified electrode for signal amplification, Electrochim. Acta. 78
439 (2012) 508-514.
440 [32] M. Hartmann, A. Vinu, G. Chandrasekar, Adsorption of vitamin E on mesoporous
441 silica molecular sieves, Chem. Mater. 17 (2005) 1169-1176.
442 [33] H. Zhen, S. Zhu, M. Hibino, I.J. Honma, Electrochemical capacitance of
443 self-ordered mesoporous carbon, J. Power Sources. 122 (2005) 219-223.

444 [34] S. Jun, S. H. Joo, R. Ryoo, M. Kruk, M. Jaroniec, Z. Liu, T. Ohsuna, O. Terasaki,
445 Synthesis of new, nanoporous carbon with hexagonally ordered mesostructure, J. Am.
446 Chem. Soc. 122 (2000) 10712-10713.
447 [35] F. Zhao, Q. Xie, M. Xu, S. Wang, J. Zhou, F. Liu, RNA aptamer based
448 electrochemical biosensor for sensitive and selective detection of cAMP, Biosens.
449 Bioelectron. 66 (2015) 238-243.
450 [36] Y.Y. Zhou, L. Tang, G.M. Zeng, C. Zhang, X. Xie, Y.Y. Liu, J.J. Wang, J. Tang, Y.
451 Zhang, Y.C. Deng, Label free detection of lead using impedimetric sensor based on
452 ordered mesoporous carbon-gold nanoparticles and DNAzyme catalytic beacons,
453 Talanta. 146 (2016) 641-647.
454 [37] J.C. Ndamanisha, L.P. Guo, Ordered mesoporous carbon for electrochemical
455 sensing: A review, Anal. Chim. Acta. 747 (2012) 19-28.
456 [38] H. Zhou, W.W. Yang, C.Q. Sun, Amperometric sulfite sensor based on
457 multiwalled carbon nanotubes/ferrocene-branched chitosan composites, Talanta. 77
458 (2008) 366-371.
459 [39] B. Bolto, J. Gregory, Organic polyelectrolytes in water treatment, Water Res. 41
460 (2007) 2301-2324.
461 [40] C. Zhang, C. Lai, G. Zeng, D. Huang, L. Tang, C. Yang, Y. Zhou, L. Qin, M.
462 Cheng, Nanoporous Au-based chronocoulometric aptasensor for amplified detection
463 of Pb(2+) using DNAzyme modified with Au nanoparticles, Biosens. Bioelectron. 81
464 (2016) 61-67.
465 [41] C. Wang, H.F. Yin, S. Dai, S.H. Sun, A general approach to noble metal-metal

oxide dumbbell nanoparticles and their catalytic application for CO oxidation, Chem. Mater. 22 (2010) 3277-3282.

[42] J. Zhang, B. Liu, H. Liu, X. Zhang, W. Tan, Aptamer-conjugated gold nanoparticles for bioanalysis, Nanomedicine 8 (2013) 983-993.

[43] M. Wilchek, E.A. Bayer, O. Livnah, Essentials of biorecognition: the (strept)avidin-biotin system as a model for protein-protein and protein-ligand interaction, Immunol Lett. 103 (2006) 27-32.

[44] A. Bini, M. Minunni, S. Tombelli, S. Centi, M. Mascini, Analytical performances of aptamer-based sensing for thrombin detection, Anal. Chem. 79 (2007) 3016-3019.

[45] Y. Xu, T. Han, X. Li, L. Sun, Y. Zhang, Y. Zhang, Colorimetric detection of kanamycin based on analyte-protected silver nanoparticles and aptamer-selective sensing mechanism, Anal. Chim. Acta. 891 (2015) 298-303.

[46] L. Qin, G.M. Zeng, C. Lai, D.L. Huang, C. Zhang, P. Xu, T.J. Hu, X.G. Liu, M. Cheng, Y. Liu, L. Hu, Y.Y. Zhou, A visual application of gold nanoparticles: Simple, reliable and sensitive detection of kanamycin based on hydrogen-bonding recognition, Sens. Actua. B: Chem. 243 (2016) 946-954.

[47] L.S. Khabbaz, M. Hassanzadeh-Khayyat, P. Zaree, M. Ramezani, K. Abnous, S.M. Taghdisi, Detection of kanamycin by using an aptamer-based biosensor using silica nanoparticles, Anal. Methods. 7 (2015) 8611-8616.

[48] N. Zhou, J. Zhang, Y. Tian, Aptamer-based spectrophotometric detection of kanamycin in milk, Anal. Methods. 6 (2014) 1569-1574.

[49] C. Li, Y.Y. Zhang, S.A. Eremin, O. Yakup, G. Yao, X.Y. Zhang, Detection of

488 kanamycin and gentamicin residues in animal-derived food using IgY antibody based
489 ic-ELISA and FPIA, Food. Chem. 227 (2017) 48-54.
490 [50] R. Li, Y. Liu, L. Cheng, C. Yang, J. Zhang, Photoelectrochemical aptasensing of
491 kanamycin using visible light-activated carbon nitride and graphene oxide
492 nanocomposites, Anal. Chem. 86 (2014) 9372-9375.
493 [51] X. Qin, W. Guo, H. Yu, J. Zhao, M. Pei, A novel electrochemical aptasensor
494 based on MWCNTs-BMIMPF6 and amino functionalized graphene nanocomposites
495 film for determination of kanamycin, Anal. Methods. 7 (2015) 5419-5427.
496
497
498
499
500
501
502
503
504

Highlights

1) An ultrasensitive electrochemical aptasensor for kanamycin (KAN) detection was constructed with a dual-signal amplification strategy.

2) DNA strand (biotin labelled) was immobilized with the biotin-streptavidin system.

3) This aptasensor shows good analytical performance in KAN analysis.